Front explosions in three-dimensional resonantly-forced oscillatory systems

Christopher J. Hemming and Raymond Kapral*
Chemical Physics Theory Group, Department of Chemistry, University of Toronto, Toronto, Ontario, Canada M5S 3H6
(Received 9 April 2003; published 7 August 2003)

Interface dynamics in a three-dimensional coupled map lattice with a period-3 local map is studied. The system possesses a parameter regime where one typically finds three-phase patterns consisting of spatially uniform domains which follow the period-3 cycle and oscillate among the three different phases. The interfaces where these domains meet may exhibit complex irregular dynamics. The system also has a parameter regime of ''turbulent'' dynamics, which is a chaotic transient with a superexponentially long lifetime. The transition from the three-phase pattern regime to the turbulent regime is studied. As a control parameter is tuned, the interfaces between domains develop turbulent structure. The thickness of the turbulent zone remains finite up to a critical parameter value after which it is infinite. We characterize this ''front explosion'' transition in three-dimensional systems and compare it with the analogous transition in two-dimensional systems where the critical properties are markedly different. The front explosion in the three-dimensional resonantly-forced complex Ginzburg-Landau equation is also investigated briefly and its character differs from that in the three-dimensional coupled map lattice.

DOI: 10.1103/PhysRevE.68.026203 PACS number(s): 05.45.−a, 89.75.Kd, 82.40.Bj

I. INTRODUCTION

If a nonlinear oscillatory medium is subjected to periodic forcing with frequency near a multiple of the natural oscillation period, the forcing may lock the phase of the oscillations to discrete values. In this circumstance, the medium exhibits patterns consisting of spatially uniform domains separated by interfaces or domain walls where the phase of the oscillation exhibits sharp jumps. Systems of this type arise in a number of different physical contexts including liquid crystals in the presence of magnetic fields [1–5], instabilities in optical systems [6–9], and oscillatory chemical media [10–13]. Such studies of resonantly-forced oscillatory media have shown that a complicated phenomenology of spatiotemporal patterns exists.

Resonantly-forced systems may be described by ''reaction-diffusion'' equations giving the time evolution of local dynamical variables $\mathbf{x}(\mathbf{r},t)$,

$$\frac{\partial}{\partial t}\mathbf{x}(\mathbf{r},t)=\mathbf{F}(\mathbf{x}(\mathbf{r},t),t)+\mathbf{D}\nabla^2\mathbf{x}(\mathbf{r},t)+\eta\mathbf{\Phi}(\mathbf{x}(\mathbf{r},t),t), \quad (1)$$

where $\mathbf{F}(\mathbf{x}(\mathbf{r},t),t)$ specifies the local dynamics, $\mathbf{D}$ is a matrix of diffusion or coupling coefficients, and $\eta\mathbf{\Phi}$ is a periodic external forcing term with amplitude η. There have been extensive studies of the resonantly-forced complex Ginzburg-Landau (CGL) equation, as well as other reaction-diffusion models, which have provided schemes to interpret the experimental studies and predicted the existence of new phenomena [14–26].

Insights into the behavior of resonantly-forced systems can be gained by studying simpler but more abstract coupled map lattice (CML) models of the form

$$s_{t+1}(\mathbf{r})=(1-2D\epsilon)f(s_t(\mathbf{r}))+\epsilon\sum_{\mathbf{r}'\in\mathcal{N}}f(s_t(\mathbf{r}')), \quad (2)$$

where $s_t(\mathbf{r})$ is the local state at the lattice site $\mathbf{r}$ at discrete time t, f is a (nonlinear) map function, D is the dimensionality of the lattice, and $\mathcal{N}$ is the von Neumann neighborhood comprising the nearest neighbors of the site $\mathbf{r}$. The parameter ϵ is proportional to the strength of the diffusive spatial coupling.

A series of investigations [27–30] of this CML model with the piecewise linear map,

$$f(s)=\begin{cases} bs, & 0\leqslant s\leqslant 1/b \\ a, & 1/b<s\leqslant 1, \end{cases} \quad (3)$$

demonstrated the existence of phenomena analogous to those seen in the resonantly-forced CGL equation. In particular, for an appropriate choice of the parameters a and b, the map has a period-3 attractor $A=a\rightarrow B=ab\rightarrow C=ab^2$, and models the behavior of a 3:1 resonantly-forced system. An especially interesting feature of the spatiotemporal dynamics in two-dimensional (2D) systems is the existence of ''turbulent'' fronts where a turbulent zone separates any two of the three homogeneous A, B, or C phases [28,29]. An example of such a turbulent interface is shown in Fig. 1 (left panel). As the system parameters are tuned, the width of the turbulent zone grows as a power law until the front ''explodes'' and the turbulent phase fills the entire domain. Similar front explosions have been shown to exist in simulations of the 3:1 resonantly-forced CGL equation [31,32], making it likely that this phenomenon can be found in the laboratory.

Analysis of the front explosion suggests that $D=3$ is a critical dimension. Consequently, it is of interest to examine turbulent front dynamics in 3D systems, and this is the aim of this paper. The outline of the paper is as follows. In Sec. II, we introduce the relevant notation and sketch the analysis of the front explosion using a stochastic model [29] that

*Electronic address: rkapral@chem.utoronto.ca

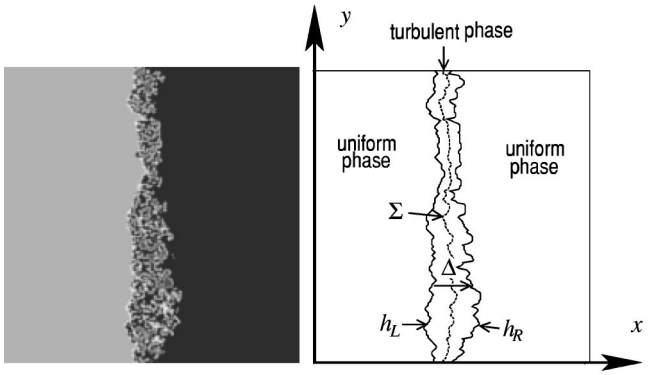

FIG. 1. (Left): Interfacial structure in the 2D CML system, Eqs. (2) and (3), for $b=2.545$, $a=0.1$, $\epsilon=0.173$. The gray scale indicates the value of the order parameter $s_t(\mathbf{r})$. System size: 200×200. (Right): Schematic depiction of the turbulent interface showing the quantities h_L, h_R, and Δ, Σ for the system configuration shown on the left.

represents the front in terms of coupled left and right profiles that separate the turbulent phase from the homogeneous phases. The structure and dynamics of turbulent fronts in the CML system in 3D geometries are discussed in Sec. III. We show that qualitative and quantitative characteristics of the front explosion differ from those in 2D geometries. The conclusions of the investigation are given in Sec. IV where comparisons with simulations of the front explosion in the CGL equation in 3D geometries are made.

II. TWO-DIMENSIONAL CML SYSTEM

The turbulent zone in the front shown in Fig. 1 (left) is separated from the homogeneous phases by left and right profiles $h_L(y,t)$ and $h_R(y,t)$, respectively, which delimit the left and right edges of the turbulent zone. Letting the value of s in the uniform phases on the left (right) be $s_0^{L(R)}$, where $s_0^{L(R)}\in\{A,B,C\}$, then $h_{L(R)}(y,t)$ is defined to be the least (greatest) value of x such that $s_t(x,y,t)\neq s_0^{L(R)}$. We define the intrinsic width of the interface as $\Delta(y,t)\equiv h_R(y,t)-h_L(y,t)$ and the mean interface profile as $\Sigma(y,t)\equiv[h_R(y,t)+h_L(y,t)]/2$. Figure 1 (right) shows these quantities for the system configuration of Fig. 1 (left). The mean intrinsic width at time t, $\overline{\Delta}(t)=L^{-1}\Sigma_{y=1}^{L}\Delta(y,t)$, fluctuates in time but is statistically stationary and has mean value Δ_0.

If one starts from initial conditions where the width of the turbulent zone is greater than the mean intrinsic width Δ_0, the homogeneous phases are observed to consume the turbulent zone and its width shrinks until Δ achieves the statistically stationary value Δ_0. Based on this observation and the front geometry in Fig. 1 (right), a coupled profile model was proposed in which the left and right Edwards-Wilkinson (EW) fronts [33,34] interact with each other via a repulsive force [29],

$$\frac{\partial h_L(\mathbf{r},t)}{\partial t}=v+\mathcal{D}\nabla^2 h_L-F_L(h_R-h_L)+\xi_L(\mathbf{r},t), \qquad (4)$$

$$\frac{\partial h_R(\mathbf{r},t)}{\partial t}=-v+\mathcal{D}\nabla^2 h_R+F_R(h_R-h_L)+\xi_R(\mathbf{r},t). \qquad (5)$$

Here, $\mathcal{D}$ and $\xi_{L(R)}$ are the diffusion coefficient and Gaussian white noise terms that appear in the EW model for a diffusively rough interface, and $F_{L(R)}$ are the repulsive forces that prevent the complete collapse of the turbulent zone. The velocity v is the mean velocity of an interface separating a semi-infinite turbulent phase from a semi-infinite uniform phase; for $v>0$, the uniform phase is more stable and propagates into the turbulent phase, while for $v<0$ the turbulent phase consumes the uniform phase. The front explosion occurs when the sign of v changes from positive to negative. For $v>0$, the system is in the confined front regime; the relative stability of the turbulent and uniform phases leads the interfacial zone to shrink. The width of the interfacial zone fluctuates about a mean intrinsic width Δ_0 determined by a balance between the contraction due to the positive sign of v and the repulsive force.

From this pair of equations, a closed evolution equation for the intrinsic width $\Delta(\mathbf{r},t)=h_R(\mathbf{r},t)-h_L(\mathbf{r},t)$ of the form

$$\frac{\partial\Delta(\mathbf{r},t)}{\partial t}=-u+\mathcal{D}\nabla^2\Delta+F(\Delta)+\xi(\mathbf{r},t) \qquad (6)$$

can be obtained [29]. Here, $u=2v$, $\xi=\xi_R-\xi_L$, and $F=F_R-F_L$. Introducing a bifurcation parameter λ and defining $\lambda>0$ to correspond to the confined regime, as $\lambda\to0^+$, Δ_0 diverges and the mean interface velocity v_f (the velocity of the mean interface Σ) vanishes. Characteristic length ℓ and time scales τ diverge at this nonequilibrium phase transition. The following critical exponents may be introduced for the behavior as $\lambda\to0^+$: α for the intrinsic width divergence, $\Delta_0\sim\lambda^{-\alpha}$; ν for the vanishing of $u=2v$, $u\sim\lambda^{\nu}$; β for the spatial scale divergence, $\ell\sim\lambda^{-\beta}$; and z for the time scale divergence, $\tau\sim\lambda^{-z}$.

Letting the dimension d of a front in a system with dimension D be $d=D-1$, one may use scaling arguments to obtain these exponents. Assuming that the repulsive force has the form $F(\Delta)=c/\Delta^{\eta}$ and requiring that Eq. (6) be invariant as $\lambda\to0^+$ leads to the following values for the critical exponents: $\alpha=[(2-d)/(2+d)]\nu$, $\beta=[2/(2+d)]\nu$, $z=[4/(2+d)]\nu$. For $d=1$, the exponents are $\alpha=\nu/3$, $\beta=2\nu/3$, and $z=4\nu/3$. If $\alpha\eta<\nu$ the force term will diverge, hence invariance requires $\eta\geqslant3\nu$. For $\eta>3\nu$, the force term renormalizes to an infinite barrier at $\Delta=0$. This model makes no prediction about the exponent ν but simulations show that $\nu=1$ for $d=1$. For the 2D CML, the measured values of the exponents α, β, and z satisfied the predictions of the coupled profile model [29].

For fronts in 3D systems, the scaling exponents are predicted to be $\alpha=0$, $\beta=\nu/2$, and $z=\nu$. Regardless of the value of η, $\alpha\eta=0$ and the force term renormalizes to become an infinite barrier at $\Delta=0$ and zero for $\Delta>0$. Thus, $d=2$ is a critical dimension for this model and it is of interest to examine the nature of the front explosion in 3D systems where the interface has dimension $d=2$.

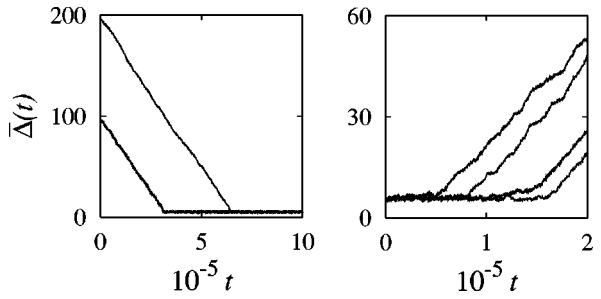

FIG. 2. $\bar{\Delta}(t)$ vs t for realizations starting from random initial conditions in the interfacial zone. System size $L=100$. Left: $b=2.5476$, initial random zone width $W=100$ and 200. Right: $b=2.548\,24$ and $W=5$.

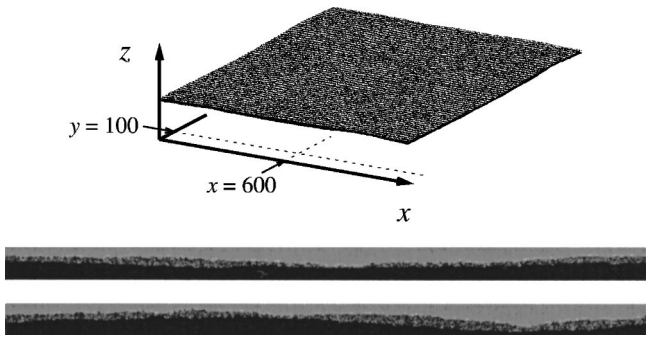

FIG. 3. A confined interfacial zone in a system with $b=2.5476$ and $L=1200$. The upper panel shows the left and right front profiles. The lower two panels are cross sections through the planes $x=600$ (middle) and $y=100$ (bottom); the horizontal scale has been compressed by a factor of 2 in these panels.

III. THREE-DIMENSIONAL CML SYSTEM

The simulations of the 3D, period-3 CML were performed keeping the parameters $a=0.1$, $\epsilon=0.117$ fixed and the control parameter b was varied. As for 2D, initial conditions were chosen where uniform regions with $s_0(\mathbf{r})$ equal to different points in the period-3 cycle of the local map f of Eq. (3) were separated by a zone of width W, where $s_0(\mathbf{r})$ takes on values randomly chosen from a uniform distribution on $[0,1]$. This initial condition rapidly relaxes to a turbulent interface with intrinsic width $\Delta \approx W$.

Consider the behavior at value $b=2.5476$. If we start from a thick initial random zone, $W=100$ or 200, the zone shrinks until the intrinsic width is small, $\bar{\Delta}(t) \approx 5-8$, after which a statistically stationary state is achieved where $\bar{\Delta}(t)$ fluctuates around a small mean value in this range. Figure 2 (left) shows some typical plots of $\bar{\Delta}(t)$ versus t for realizations at this parameter value. For the 3D system, the front propagation is chosen to be in the z direction and the functions h_L, h_R, Σ, and Δ depend on the spatial variables x and y as well as time. We continue to refer to h_L as the left profile and h_R as the right profile even though in figures we show the z-axis pointing in the upwards direction. The statistically stationary state, where the interfacial zone is thin and confined, is also reached from initial conditions with a thin random zone with $W=5$. Figure 3 shows a typical thin interface for $b=2.5476$.

A. Transient behavior and front collapse

In the 2D CML, collapse of turbulent fronts to periodic attractors was observed for small system sizes [28]. The periods of these attractors could be quite large and the particular attractor to which the collapse occurred depended on the initial conditions. The average time for collapse to a periodic attractor was found to depend superexponentially on the linear system dimension, $\tau_c \sim e^{c_1 L^{1.5}}$ where c_1 is a constant [28]. Consequently, although the rough fronts observed in these systems are simply transients, for sufficiently large system sizes they are the only physically relevant states. A similar exponential dependence on the system size was found in 1D systems [27]. The CML model also exhibits stable chaos [27,35,36] since the largest Lyapunov exponent is negative for the turbulent state, although this state has all the other characteristics of deterministic chaos such as rapid decay of correlations in space and time.

In 3D systems with small spatial extent normal to the propagation direction, the thin $d=2$ interface eventually collapses to a more regular state in which the intrinsic width $\Delta_0 \approx 4$. Figure 4 (left) shows $\bar{\Delta}(t)$ versus t for a realization in which this collapse happens. While we have not attempted to determine if the collapsed state in the 3D system is periodic, it is clear that the interface dynamics in the collapsed state are much simpler than in the confined turbulent state. The average lifetime of the turbulent state before collapse, τ_c, is shown as a function of L in Fig. 4 (right) for a fixed value of $b=2.5476$. We find that τ_c increases with system size as $\tau_c \sim e^{c_2 L^{2.56}}$.

This behavior suggests that we can imagine the turbulent zone as being made up of some number $N(L)$ of independent randomly evolving domains within which the spatiotemporal dynamics is strongly correlated. At the collapse point, the $N(L)$ random processes must simultaneously take on the same value; hence $\tau_c \sim e^{N(L)}$. The number of such statistically independent domains should scale with the system size as $N(L) \sim L^{d+\zeta}$ since the interface area in the dimensions transverse to the front propagation direction increases as L^d and the contribution L^ζ arises from the effective thickness of the interface, depending on both the intrinsic width of the

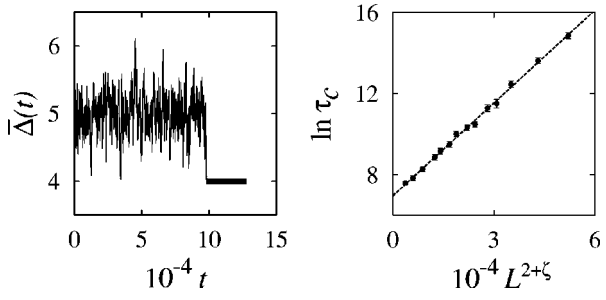

FIG. 4. Left: Intrinsic width $\bar{\Delta}(t)$ vs t for a realization in which the collapse from the confined turbulent state occurs. Parameters: $b=2.5476$, system size $L=55$; Right: Plot of $\ln \tau_c$ against $L^{2+\zeta}$, where $\zeta=0.56$, with $b=2.5476$. The dashed best-fit line is $\ln \tau_c = 1.52\times 10^{-4}\times L^{2+\zeta}+6.96$.

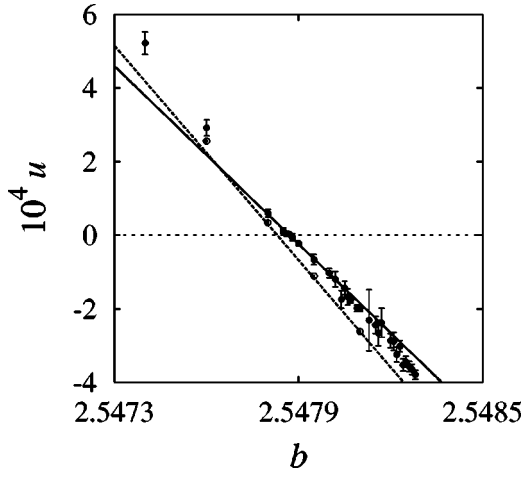

FIG. 5. Interface velocity u vs b in systems of size $L=100$ (filled circles) and $L=800$ (open circles). The solid line is $u=-0.805\,259\times(b-2.547\,87)$; this is the linear term of a cubic polynomial fit to the $L=100$ data in the interval $2.5478\leqslant b\leqslant 2.548$. The dashed line has equation $u=-0.970\,98\times(b-2.547\,83)$ and is the linear term of the cubic fit to the $L=800$ data. The dotted line indicates $u=0$.

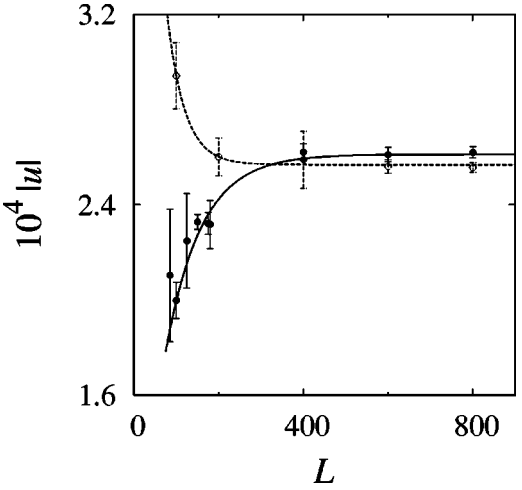

FIG. 6. Dependence of $|u|$ on system size L for $b=2.5481$ (filled circles) and $b=2.5476$ (open circles). For $b=2.5481$, $u<0$; for $b=2.5476$, $u>0$. The smooth curves plotted through the data are guides to the eye.

interface and the roughness of the profile.

These results show that the transient turbulent fronts with superexponentially long lifetimes are the relevant system states also in sufficiently large 3D systems.

B. Front explosion in 3D

From observations of the contraction of the interfacial zone like those shown in Fig. 2 (left), the mean contraction velocity $u=-\langle d\overline{\Delta}/dt\rangle$, where the average $\langle\cdot\rangle$ is taken over time and realizations of the evolution process, may be determined. With this definition, u has the same meaning as in Eq. (6) of the coupled profile model. Measuring u as a function of b at a fixed system size L, we see in Fig. 5 that as b increases, the contraction rate u passes through zero at $b^*(L)$. For $b>b^*(L)$, the turbulent zone grows rather than shrinks. Figure 2 (right) shows typical $\overline{\Delta}(t)$ versus t curves for a few realizations at a b value within the expanding interface regime where $b>b^*(L)$ and $u<0$. As for a contracting interfacial zone, u can be estimated from the linear growth of $\overline{\Delta}(t)$.

From Fig. 5, we find $b^*(100)\simeq 2.547\,87$ and $b^*(800)\simeq 2.547\,83$ indicating a weak dependence on L. To further investigate the system size dependence, Fig. 6 plots $|u|$ versus L for two values of b in the contracting and expanding regimes. For $L>400$, $|u|$ is independent of L showing that, for large enough systems, an L-independent critical value b^* can be defined.

Since $u<0$ for $b>b^*(L)$, the intrinsic width $\overline{\Delta}(t)$ will grow without bound. Consistent with this, in simulations, we see no sign of saturation of the intrinsic width when $u<0$. Figure 7 shows the typical structure of an expanding interfacial zone.

One can see in Fig. 2 (right) that the state where $\overline{\Delta}(t)$ grows linearly in time is preceded by a transient confined state in which $\overline{\Delta}(t)\approx 5$–$8$ and fluctuates around an average value Δ_m. We define the lifetime τ_m of this metastable confined state to be the largest t for which $\overline{\Delta}(t)=8$, a value slightly larger than the mean intrinsic width Δ_m. We let $\overline{\tau_m}$ be the average of τ_m over realizations. The average lifetime $\overline{\tau_m}$ decreases as b increases and we move farther into the expanding regime (Fig. 8, right). For b only slightly greater than $b^*(L)$, the lifetime of the metastable confined state can be quite long [37]. As the system size increases, $\overline{\tau_m}$ decreases (Fig. 8, left).

The fact that $d\overline{\Delta}(t)/dt$ does not depend on $\overline{\Delta}(t)$ for sufficiently large front profile separations suggests that there is no interaction between the left and right profiles for large distances. The center of mass position of the mean front profile $\overline{\Sigma}(t)=L^{-2}\Sigma_{x,y=1}^{L}\Sigma(x,y,t)$ can have a nonzero net velocity only when the left and right profiles interact. Figure 9 shows $\overline{\Delta}(t)$ and $\overline{\Sigma}(t)$ versus t for a realization of the front

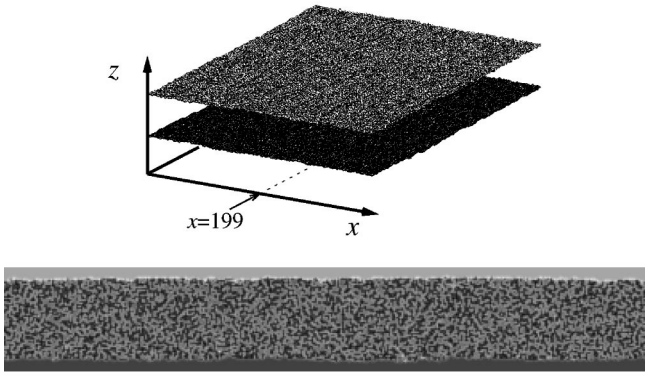

FIG. 7. The interfacial zone in a system with $b=2.5479$ and $L=400$. The upper panel shows the left and right interface profiles. The arrow indicates the plane $x=199$. The lower panel is a cross section through this plane.

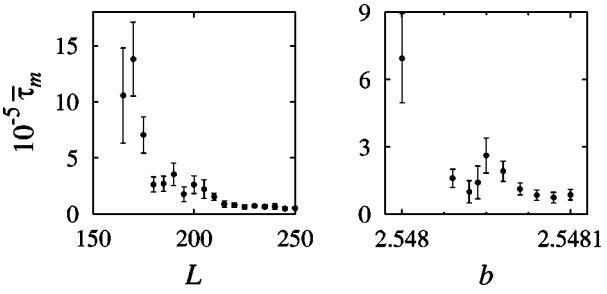

FIG. 8. Left: Dependence of the mean lifetime of the confined state, $\overline{\tau_m}$ on system size L in simulations with $b=2.548\,05$. Right: Dependence of $\overline{\tau_m}$ on the parameter b for system size $L=200$.

evolution process. We see that in the metastable confined state, the average center of mass velocity is a nonzero value, but when the transition to the state of linear expansion occurs, the average center of mass velocity falls to zero.

For the 2D CML, the intrinsic width Δ_0 diverges as $b \to b^{*-}$. In contrast, for the 3D CML, the transition is discontinuous, at least for finite system sizes: Δ_0 remains finite for $b \leqslant b^*(L)$ and infinite for $b > b^*(L)$. For $b > b^*(L)$, it is possible to measure the average of Δ in the metastable confined state, Δ_m. Figure 10 shows Δ_0 and Δ_m as a function of b. The results in this figure demonstrate that the character of the front explosion is qualitatively different in the 2D and 3D CML systems, and this is one of the important observations of this study.

C. L dependence of interfacial properties

The coupled profile model used to analyze the front explosion was based on the observation that the interfaces that separated the turbulent zone from the homogeneous phases satisfied EW scaling [29]. The interfacial profile widths are defined as

$$\langle w_I \rangle(t) = \left\langle L^{-d} \left(\sum_{(x,y)} (h_I(x,y,t) - \overline{h_I}(t))^2 \right)^{1/2} \right\rangle, \qquad (7)$$

where $I = L,R$, the sums are taken over all (x,y),

$$\overline{h}(t) = L^{-d} \sum_{(x,y)} h_I(x,y,t) \qquad (8)$$

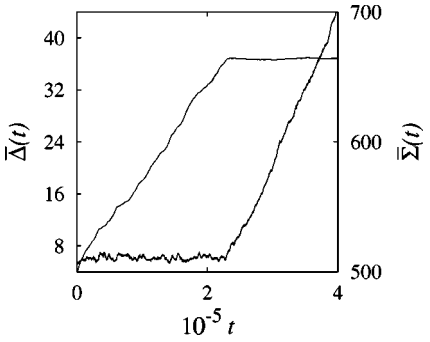

FIG. 9. Plot of $\overline{\Delta}(t)$ (lower curve, left-hand ordinate) and the center-of-mass position $\overline{\Sigma}(t)$ (upper curve, right-hand ordinate) vs t for a realization in a system of size $L=150$ with $b=2.5481$.

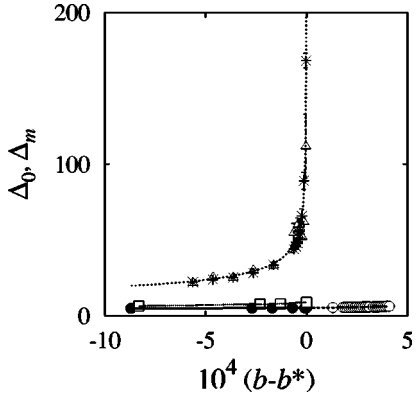

FIG. 10. Average intrinsic width Δ_0 vs $b-b^*(L)$ in the confined regime $b<b^*(L)$, and average intrinsic width Δ_m for the metastable confined state in the expanding regime $b>b^*(L)$, where $b^*(L)$ is the critical parameter value for the front explosion transition. Values for 3D systems with $L=100$, for which $b^*(100)=2.547\,87$, are shown by filled circles for $b<b^*(100)$ and by open circles for $b>b^*(100)$ while data for $L=800$, for which $b^*(800)=2.547\,83$, are shown as open squares. Values for 2D systems with $L=100$ (open triangles) and $L=800$ (asterisks), for which $b^*=2.545\,662$ (independent of L) are also shown for comparison. Smooth curves have been fit through the 3D data as guides to the eye; the fit to the two-dimensional data indicates power law divergence with exponent $-1/3$.

is the mean profile position at time t for a particular realization, and the average $\langle \cdot \rangle$ is taken over realizations. The leading (right) profile widths $\langle w_R \rangle$ for b in the expanding (E) and contracting (C) regimes are plotted in Fig. 11 as a function of L. For comparison, we also show the corresponding width

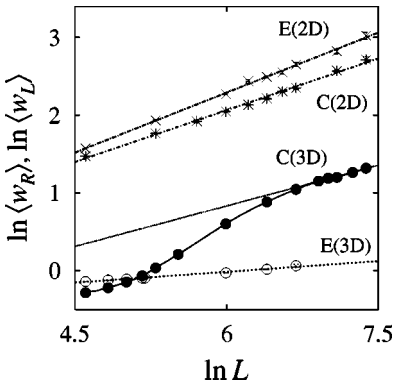

FIG. 11. Plot in logarithmic coordinates of the average width of the leading interface profile against system size L. The curves are labeled indicating the system's dimensionality, and whether the b value lies within the confined (C) or expanding (E) regime. For 3D systems, $\langle w_R \rangle$ is shown for the parameter values $b=2.5476$ [C(3D), filled circles] and $b=2.5481$ [E(3D), open circles]. A smooth curve is plotted as a guide to the eye for the C(3D) data. The straight lines have slopes 0.35 and 0.09, respectively, for these two parameter values. The C(3D) straight line is obtained from a fit to the data for $L \geqslant 1000$. For two-dimensional systems, $\langle w_L \rangle$ is shown for $b=2.545$ [C(2D), asterisks] and $b=2.54575$ [E(2D), crosses]. The straight lines have slopes 0.51 and 0.44, respectively, for these two parameter values.

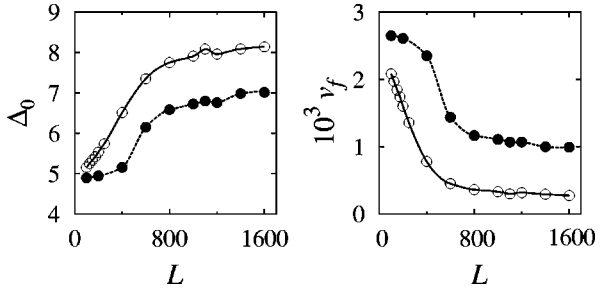

FIG. 12. Dependence on system size L for mean intrinsic width Δ_0 (left) and center-of-mass velocity v_f (right). Data are shown for $b=2.547$ (filled circles) and $b=2.5476$ (open circles). Errorbars on data points are smaller than the marker circles. The curves plotted through the data are guides to the eye.

data for 2D systems. The profile width data for 3D confined fronts [C(3D)] show a crossover, for system sizes larger than approximately $L=600$, to a scaling form $\langle w_R\rangle \sim L^{0.35}$, which is close to the exponent of 0.38 for Kardar-Parisi-Zhang (KPZ) fronts in 3D ($d=2$) systems [38,39]. The 2D data [C(2D)] show no such evidence of a crossover in this system size range. In contrast, the expanding front profile widths [E(3D)] show a very weak power law behavior $\langle w_R\rangle \sim L^{0.09}$, reasonably close to the EW prediction of $\ln L$ behavior. In summary, for 2D systems, in the chosen parameter range, the front profiles approximately satisfy EW scaling in both the confined and expanding front regimes. For 3D systems, the front profiles in the expanding regime satisfy EW scaling approximately; however, the profiles of the confined fronts show strong L dependence with a crossover to approximate KPZ scaling for large L. These results signal a change in behavior for $d=2$ as predicted by the coupled profile model but the results further indicate that the EW coupled profile model should lose its validity for the $d=2$ confined fronts in 3D systems.

The intrinsic width of the confined fronts in the 3D system has only a weak dependence on the bifurcation parameter (see Fig. 10). However, like the profile width, the intrinsic width exhibits a strong L dependence and crossover behavior. The mean intrinsic interface width Δ_0 and the center of mass interface velocity v_f were measured as functions of system size L (Fig. 12, left and right panels, respectively) for two values of b for which confined interfaces exist. Each of these properties shows different behaviors at small and large system sizes, with the crossover between the two regimes occurring at $L\approx 600$.

Whether or not, there is a phase transition between confined and exploding interface regimes in the limit $L\to\infty$ depends on whether $\lim_{L\to\infty}\Delta_0$ is finite. The results presented in Fig. 12 (left) do not allow a definitive prediction as to whether Δ_0 remains bounded or diverges as L becomes large. In numerical simulations of Eq. (6) of the coupled profile model, where the repulsive force F is taken to be a hard wall repulsion,

$$F(\Delta)=\begin{cases}\infty, & \Delta\leqslant 0\\ 0, & \Delta>0,\end{cases} \tag{9}$$

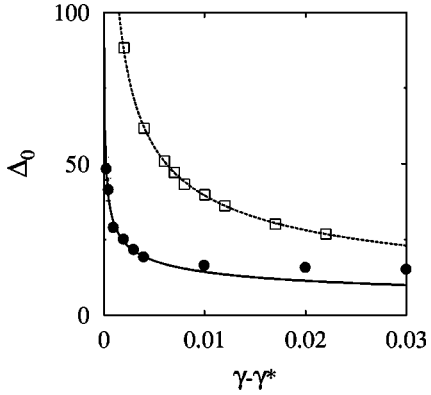

FIG. 13. Average intrinsic width Δ_0 vs $\gamma-\gamma^*$ for the 2D 3:1 forced complex Ginzburg-Landau equation (hollow squares) and 3D (filled circles). For 2D, $\gamma^*=0.458$, for 3D, $\gamma^*=0.520$. The smooth curves represent power law divergence with exponents -0.49 for 2D and -0.33 for 3D. The exponent for the 3D curve is obtained from a fit to the data for $\gamma-\gamma^*\leqslant 0.005$.

the average intrinsic width $\Delta_0=\langle\Delta\rangle$, where $\langle\cdot\rangle$ is a spatiotemporal average, is independent of L as L becomes large. The left and right profiles in the CML do not interact when their separation is sufficiently large, and therefore this model should capture the essential features affecting the boundedness or divergence of Δ_0 as L becomes large. This model predicts that Δ_0 remains bounded as $L\to\infty$.

IV. CONCLUSIONS

The manner in which the front explosion occurs in the 3D period-3 CML system is qualitatively different from that in 2D systems. In 2D, the interface width diverges according to a power law as the transition point is approached from the confined front side of the bifurcation, but in 3D, for a fixed system size, the front explosion transition occurs directly from a finite value of $\Delta_0(L)$. If the intrinsic width remains finite as $L\to\infty$, as suggested by the analysis of the 3D coupled profile model, one expects a first-order phase transition in this limit in contrast to the continuous transition observed in the 2D CML.

The scaling properties of the front explosion were investigated for the 2D 3:1 resonantly forced Ginzburg-Landau equation in the Benjamin-Feir unstable regime [31,32]. Although the scaling exponents differed, both the 2D period-3 CML and 2D 3:1 forced CGL systems showed similar front explosion phenomenology and, in particular, power law divergence of the intrinsic width. Consequently, it is interesting to compare the results obtained in this study with the corresponding front explosion phenomenon in the 3D 3:1 forced CGL system. Simulations of the front explosion are lengthy, requiring large 3D system sizes and long integration times to carry out the statistical averages. Consequently, our results are limited in scope. Figure 13 shows the results of such simulations for the 3D 3:1 forced CGL equation carried out for a system with a turbulent front propagating along the z direction. As in earlier studies in 2D [31,32], a moving frame with no-flux boundary conditions along z and periodic boundary conditions along x and y was used. Simulations

were carried out for a single system size with linear dimension $L=50$ along x and y. The results of an earlier 2D study, carried out in systems of size $L=200$, are also shown in the figure for comparison. In contrast to the CML results which indicate a different front explosion character in 2D and 3D dimensions, the 3:1 forced CGL results show power law divergence as a function of the forcing intensity γ in both 2D and 3D, although the exponents are different [$\Delta_0 \sim (\gamma - \gamma^*)^{-0.49}$ and $\Delta_0 \sim (\gamma - \gamma^*)^{-0.33}$ in 2D and 3D systems, respectively]. These differences are likely due to the different nature of the correlations in the turbulent state in the CML and forced CGL systems as well as the fact that the front profiles separating the turbulent and homogeneous states also have different character, exhibiting EW scaling for the CML and KPZ scaling for the forced CGL equation.

The CML system and the forced CGL equation share general qualitative features but differ in other respects such as the nature of the nonlinearity giving rise to turbulence. The turbulent state in the CML possesses a negative maximal Lyapunov exponent, while in forced CGL equation the maximal Lyapunov exponent associated with the turbulence is positive, although the 2D results suggest that this difference does not affect the existence of the front explosion phenomenon. Both the systems possess both a turbulent state and a spatially uniform state which is stable to inhomogeneous perturbations. When the relative stability of these two states changes, the front explosion occurs.

The results of this study should provide additional stimulus for further investigations, both theoretical and experimental, of the nature of nonequilibrium phase transitions in resonantly forced oscillatory media. Since 2:1, 3:1, and 4:1 resonantly forced reaction-diffusion systems have been investigated experimentally [11–13], these systems are likely candidates for the observation of turbulent fronts.

ACKNOWLEDGMENT

This work was supported in part by a grant from the Natural Sciences and Engineering Research Council of Canada.

[1] T. Frisch, S. Rica, P. Coullet, and J.M. Gilli, Phys. Rev. Lett. **72**, 1471 (1994).
[2] P. Coullet, J. Lega, B. Houchmanzadeh, and J. Lajzerowicz, Phys. Rev. Lett. **65**, 1352 (1990).
[3] T. Kawagishi, T. Mizuguchi, and M. Sano, Phys. Rev. Lett. **75**, 3768 (1995).
[4] J. Lee, J. Kim, G.-.H. Yi, and K.J. Lee, Phys. Rev. E **65**, 046207 (2002).
[5] S. Nasuno, N. Yoshimo, and S. Kai, Phys. Rev. E **51**, 1598 (1995).
[6] P. Coullet and K. Emilsson, Physica A **188**, 190 (1992).
[7] D. Michaelis, U. Peschel, F. Lederer, D.V. Skryabin, and W.J. Firth, Phys. Rev. E **63**, 066602 (2001).
[8] S. Longhi, Phys. Rev. E **63**, 055202(R) (2001); Phys. Rev. A **65**, 045802 (2002).
[9] G. Izús, M. San Miguel, and M. Santagiustina, Phys. Rev. E **64**, 056231 (2001).
[10] V. Petrov, Q. Ouyang, and H.L. Swinney, Nature (London) **388**, 655 (1997).
[11] A.L. Lin, V. Petrov, H.L. Swinney, A. Ardelea, and G.F. Carey, in *Pattern Formation in Continous and Coupled Systems; The IMA Volumes in Mathematics and Its Applications*, edited by M. Golubitsky, D. Luss, and S. H. Strogatz (Springer, New York, 1999), Vol. 115, p. 193.
[12] A.L. Lin, A. Hagberg, A. Ardelea, M. Bertram, H.L. Swinney, and E. Meron, Phys. Rev. E **62**, 3790 (2000).
[13] A.L. Lin, M. Bertram, K. Martinez, H.L. Swinney, A. Ardelea, and G.F. Carey, Phys. Rev. Lett. **84**, 4240 (2000).
[14] V. Petrov, M. Gustaffson, and H.L. Swinney, in *Proceedings of the 4th Experimental Chaos Conference: August 6-8 1997, Boca Raton, Florida, USA*, edited by M. Ding, W. Ditto, L. Pecora, S. Vohra, and M. Spano (World Scientific, Singapore, 1998).
[15] P. Coullet and K. Emilsson, Physica D **62**, 119 (1992).
[16] C. Elphick, A. Hagberg, and E. Meron, Phys. Rev. Lett. **80**, 5007 (1998); Phys. Rev. E **59**, 5285 (1999).
[17] P. Coullet, T. Frisch, and G. Sonnino, Phys. Rev. E **49**, 2087 (1994).
[18] D. Battogtokh and D.A. Browne, Phys. Lett. A **266**, 359 (2000).
[19] D.J. Wielaard and G.S. Triantafyllou, Physica D **90**, 197 (1996).
[20] H. Chaté, A. Pikovsky, and O. Rudzick, Physica D **131**, 17 (1999).
[21] R. Gallego, D. Walgraef, M. San Miguel, and R. Toral, Phys. Rev. E **64**, 056218 (2001).
[22] J. Kim, J. Lee, and B. Kahng, Phys. Rev. E **65**, 046208 (2002).
[23] T. Mizuguchi and S. Sasa, Prog. Theor. Phys. **89**, 599 (1993).
[24] H.-K. Park, Phys. Rev. Lett. **86**, 1130 (2001).
[25] P. Coullet and K. Emilsson, in *Instabilities and Nonequilibrium Structures V*, edited by E. Tirapegui and W. Zeller (Kluwer Academic Publishers, Dordrecht, 1996), p. 55.
[26] C.J. Hemming and R. Kapral, Chaos **10**, 731 (2000).
[27] A. Politi, R. Livi, G.-L. Oppo, and R. Kapral, Europhys. Lett. **22**, 571 (1993).
[28] R. Kapral, R. Livi, G.-L. Oppo, and A. Politi, Phys. Rev. E **49**, 2009 (1994).
[29] R. Kapral, R. Livi, and A. Politi, Phys. Rev. Lett. **79**, 2277 (1997).
[30] Y. Cuche, R. Livi, and A. Politi, Physica D **103**, 369 (1997).
[31] C.J. Hemming and R. Kapral, Faraday Discuss. **120**, 371 (2002).
[32] C.J. Hemming and R. Kapral, Physica D **168**, 10 (2002).
[33] S.F. Edwards and D.R. Wilkinson, Proc. R. Soc. London, Ser. A **381**, 17 (1982).
[34] Simulations on the $d=1$ CML model showed that the left and right fronts satisfied Edwards-Wilkinson scaling for the system sizes investigated ($L=100$–1000). Crossover to KPZ scaling was estimated to occur at $L \approx 17\,000$.

[35] J.P. Crutchfield and K. Kaneko, Phys. Rev. Lett. **60**, 2715 (1988).

[36] F. Ginelli, R. Livi, and A. Politi, J. Phys. A **35**, 499 (2002).

[37] It appears that $\overline{\tau}_m$ does not decrease to zero as L increases but rather tends to a minimum value $\overline{\tau}_m \approx 5 \times 10^4$. This is a result of the definition of $\overline{\tau}_m$: a finite time is required for $\overline{\Delta}$ to grow from its initial value of approximately 5 to $\overline{\Delta} = 8$.

[38] H.L. Barabási and H.E. Stanley, *Fractal Concepts in Surface Growth* (University of Cambridge, New York, 1995).

[39] M. Kardar, G. Parisi, and Y.-C. Zhang, Phys. Rev. Lett. **56**, 889 (1986).